Photophysics of Single PPV Derivative Polymers

J. J. Liang[a] (梁君致), J. H. Hsu[b] (徐瑞鴻),
T. S. Lim[c] (林宗欣) and Jonathon David White[d]* (白小明)
[a]*Dept. of Physics, Fu Jen Catholic University, Taipei, Taiwan, R.O.C.*
[b]*Dept. of Material Science and Opto-electronic Science, National Sun Yat-sen University, Kaohsiung, Taiwan, R.O.C.*
[c]*Dept. of Physics, Tunghai University, Taichung, Taiwan, R.O.C.*
[d]*Dept. of Photonics Engineering, Yuan Ze University, Chung-Li, Taiwan, R.O.C.*

Conjugated polymers are unique subjects composed of many excitons localized at individual segments. Migration of excitation is strongly correlated with the chain conformation. We studied the PPV derivative polymers, MEH-PPV and DOO-PPV, with different chain lengths to probe the relation between the conformation of, and exciton migration in, single polymers. Photo-quenching of individual conjugated segments was used to provide information on the exciton migration process. A phenomenological model based on the polymer as a collection of conjugated segments has been developed to explain the observation. The purpose of this paper is not to provide an exhaustive account of research in the field but rather to emphasis the unique contributions of the group of Prof. W. S. Fann.

Keywords: Single molecule spectroscopy; Conjugated polymers; Excitons; Photo-quenching.

1. INTRODUCTION

Luminescent conjugated polymers have been the focus of extensive research due to their potential application as the active layer in plastic light emitting diodes and solar cells. This is due to the fact that low-cost chemical processing techniques can be used to optimize the band gap of these semiconducting polymers for either absorption or emission for the required application. In flat panel displays, the fact that these polymers are self-luminescent offers the potential of higher efficiency relative to conventional LCD displays due to the elimination of back-lighting along with an increased viewing angle. Despite the technological importance of these linear macromolecules, the fundamental photo-physics of these molecules are complicated. As such they have been the focus of considerable research both in solution and thin film forms.

Within conjugated polymer films a number of different types of excitations can exist, the most common of which are called excitons – of which two kinds have been identified. The first type is denoted as *intrachain* excitons that results from the first extended π-conjugation along the polymer backbone (Fig. 1-a yellow region). The second type is denoted as *interchain* excitons which arise from the coupling through space of two or more adjacent chain segments (e.g. Fig. 1-a purple region). This coupling can be either between segments of different chains or segments of the single chain that has folded back on itself.

While a number of competing models seek to explain the observed photo-electrical properties of these polymers, for the sake of the presentation here, we will concentrate on the molecular exciton model[1] to provide a framework to understand the nature of intrachain *excitons* in a single extended chain. Within an extended chain, interrupted conjugation, e.g. due to chain twisting or single bonds substituting double bonds, results in the chain being divided into a number of conjugated segments, also called chromophores, each of which can potentially absorb and emit light – the wavelength of which is proportional to the conjugation length as shown schematically in Fig. 1-b. Unfortunately while the models (at least those coming from the exciton point of view) describe what is expected in a single extended chain, it is difficult to verify models due to the information loss inherent in ensemble measurements. It was thus that in the late 1990's Prof Fann's group turned to the newly developing field of single molecule spectroscopy* to investigate the nature of these chromophores and the in-

Dedicated to the memory of Professor Wunshain Fann (1961–2008).

* In single molecule spectroscopy, the concentration of the molecule in questions is reduced so that only one molecule or object is observed at one time.

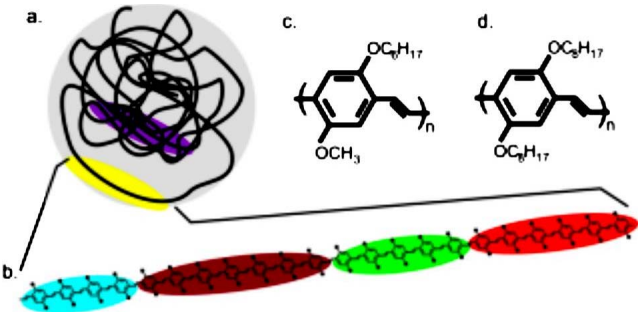

Fig. 1. Physical and chemical structure of PPV derivative conjugated polymers (a) Conformation of a long chain polymer (b) Molecular exciton model of an isolated (no interchain interactions) extended section of the polymer chain. The chain is composed of a number of static (for time scales > 1 ps) conjugated segments or chromophores whose band gap is inversely proportional to conjugation length. As chain length increases the polymer, as seen in (a), can loop back on itself opening up pathways for both 1 (intrachain) and 3 dimensional (interchain) exciton migration. (c) Chemical structure of non-symmetric MEH-PPV (d) Chemical Structure of symmetric DOO-PPV.

teraction, i.e., non-coherent energy transfer, between them. (Coherent energy transfer, occurring on the femtosecond timescale,[2] is outside of the field of this investigation)

Among the luminescent conjugated polymers, one particular family, that of PPV derivative polymers has received particular attention. Fann's group has focused on understanding two prominent and related members of the family: poly[2-methoxy-5-(2′-ethyl-hexyloxy)-1,4-phenylene vinylene] (MEH-PPV) (Fig. 1-c) and poly[2,5-dioctyloxy (p-phenylene-vinylene)] (DOO-PPV, alternatively denoted as DO-PPV) (Fig. 1-d). These molecules were chosen due to their potential for technological application in organic light-emitting diodes and photovoltaics and for the fact that one is symmetric and the other asymmetric with respect to their side-groups. Even at that early time, Fann was aware that the properties of conjugated polymers are not simply determined by the functional groups, but are also chain-length dependent.[3] Thus, in contrast to the approach of other groups which directly investigated long chain polymers,[4,5] Fann directed us to initially concentrate on short rod-like chains in order to understand intrachain excitons or chromophores without the complications of three dimensional energy transfer or interchain excitons, and then, based on this understanding, to investigate longer chains containing hundreds of chromophores. While other groups concentrated on seeking to reduce or eliminate quenching, Fann's group took the opposite approach, making use of photo-quenching events to shed light on photo-physics and exciton migration in single polymers.

2. EXPERIMENTAL

2.1. Sample Preparation

Polymers (MEH-PPV (M_n~4kDa, $\delta = 1.8$),[6] DOO-PPV (M_n~8kDa, $\delta = M_w/M_n = 2.23$, ~24 monomers),[7,8] MEH-PPV (M_w = 500 kDa, ~1800 monomers),[9] DOO-PPV (M_w = 1300 kDa, $\delta = 4.0$)[10]) were first prepared and then dried to allow long term storage. Immediately prior to spin coating, the polymer was redissolved into a "good" solvent, i.e., chloroform (in some of the work reported in,[9] toluene was used), to a final concentration of $<10^{-4}$ M of monomer. (In this case, a "good" solvent has the meaning of a solvent in which the polymer readily dissolves.) As the polymer is not very stable in chloroform, fresh solutions were used. The sample was then further diluted (by factors of 10^3 to 10^6) in an inert polystyrene (PS) matrix (typically polystyrene: chloroform: toluene = 5mg:8mL:2mL). As oxygen is extremely efficient quencher of fluorescence, dry-N_2 was bubbled through all solutions to purge dissolved oxygen from the solution. The solution was then spin-cast onto a fused silica cover slip substrate (Esco Products) to form a film thickness of <100 nm containing ~20 of the polymeric molecules of interest in a 100 μm^2 region. Samples were then placed in a dry nitrogen environment and allowed to dry under low pressure for a number of hours. Finally the pressure was raised to atmospheric pressure and placed in a specially designed holder (Fig. 2-g) to protect from oxygen and moisture during scanning.[11]

2.2. Microscope Setup

a. Basic Configuration

The basic configuration of the single molecule microscope, built around a standard optical microscope (Nikon Ellipse 660) whose illumination optics were removed is shown in Fig. 2-a.[12] The sample holder was screwed into an adapter plate connected to a closed-loop two dimensional piezo-electric scanning stage (Physik Instrumente P-730, Fig. 2-g) mounted on the microscope stage. The output of the laser source after passing through a narrow band filter (NB), was reflected by a dichroic beam splitter (DM) mounted in the microscope's filter cube and focused to a 0.16 μm^2 spot at the sample plane by the microscope's ob-

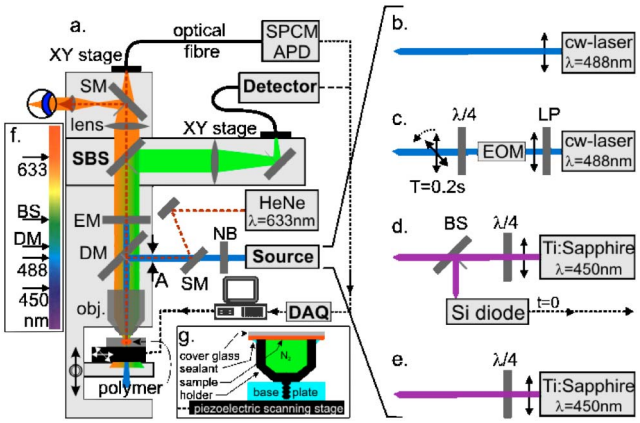

Fig. 2. (a) Basic elements of the sample scanning confocal microscope used for the experiments. (b) Laser source used for taking time traces and monitoring spectral change on the millisecond time scale. (c) Modification of excitation to allow the orientation of absorbing chromophores to be monitored. (d) Modification of excitation to measure PL lifetime (e) Excitation source for fluorescence correlation experiments (f) Spectral schematic showing the spectral locations of the laser sources and filters used in the experiments (g) Cell for mounting and protecting the sample from oxygen and water vapor during scanning.

jective lens (Nikon 100X oil immersion, N.A. = 1.3, infinity focus), The beam diameter (ϕ = 6 mm) was chosen to slightly underfill the back of the objective (obj.) to minimize self-fluorescence. The fluorescence was collected through the same objective and directed back through the dichroic mirror (DM). A long pass filter (EM) was used to block reflected light from the excitation source. After passing a sliding beam splitter (SBS), located in the double port accessory of the Nikon microscope, fluorescence was focused (by the f = 200 mm tube lens of the microscope) onto an optical fiber (PerkinElmer) placed in a XY-stage assembly (ThorLabs ST1XY-A (XT-stage) + SM1FC (FC fiber connector) + SM1LTRR retaining ring) on the microscope's camera mount. Upon exiting the fiber, the light was refocused onto an APD (PerkinElmer SPCM-AQ-13/14/15, dark-count ~15-100 cps depending on model, η_{QE} ~ 65% in the region of interest) operating in single photon counting mode. The output of the detector was fed into a computer via a data acquisition card (DAQ). Computer software, written in LabVIEW (National Instruments) was used to control the motion of the stage and collection of data. Two sliding mirrors (SM) allowed an additional HeNe laser (λ = 633 nm), aligned co-axially to the excitation laser, to be used during system alignment to ensure that the sample was located in the focal plane of the objective and reflected beams focused on the fiber aperture. After determining the positions of single polymers by raster scanning the sample under low irradiance, the excitation beam was fixed on individual polymers, power increased to 200~1600 W/cm^2 and the photoluminescence or fluorescence (PL) observed. Changing the laser source, DAQ card, and using the SBS to direct light to a second detector allowed numerous single molecule experiments could be performed as will be explained below. Fig. 2-f summarizes the wavelengths of the lasers and filters used in the experiments described in this paper.

b. Specific Configurations

For measuring the PL time trace the linearly polarized TEM_{00} mode of an Ar-Ion laser (λ_{excite} = 488 nm, chosen to be near the absorption maximum of the polymers being studied) was used as the excitation source (Fig. 2-b), Omega Optical filter 515DRLP was used for DM, Omega Optical 520EFLP for EM and the SBS transmission was set to 100%, i.e., mirror out. A standard counter/timer PCI card (National Instruments PCI-6602) was used for DAQ allowing intensity changes to be measured with 10 ms accuracy.

In order to measure the single molecule PL spectra, the EM filter was removed and the SBS reflection set to 100%, i.e., mirror in. As in the basic setup, emission was focused onto a fiber but instead of being coupled into an APD, the fiber was attached to an Acton Research 0.25 M monochromator. Light exciting the spectrograph was detected using a liquid N2 cooled CCD (Princeton Instruments).

In order to obtain information on the time evolution of an individual polymer's PL spectrum, it is necessary to split the emission into discrete channels as the S/N ratio in single molecule experiments is not high enough for the complete spectra to be recorded with 10 ms time resolution. To this end, the SBS was replaced by a polarization insensitive beam-splitter (λ_{center} = 555 nm, BS in Fig. 2-f). Two calibrated APDs (APD_g detecting from 520 nm to 555 nm and APD_r detecting from 555 nm to 675 nm) were used to record the PL time traces. The normalized spectral shift coefficient, S, defined as:

$$S(t) = \frac{I_r(t) - \gamma I_g(t)}{I_r(t) + \gamma I_g(t)} \quad (1)$$

where $I_{g(r)}$ is the intensity recorded by the APD monitoring

the green(red) portion of the spectra and γ is the ratio of the detector efficiencies. If the PL spectrum does not change with time, $S(t)$ will be constant with time. A gradual change will appear as a slanted line and a sudden spectral jump by a discontinuity. For example, if a chromophore with a slightly blue-shifted spectrum (with respect to other emitting chromophores) stops emitting, $S(t)$ will suddenly increase. This calculation and conclusion is independent of the calibration of the two collection channels.

The conformation of a polymer was probed by slowly rotating the polarization of the CW excitation light (Fig. 2-c). Excitation light was passed, in order, through a linear polarizer (LP), an electro-optical modulator (Conoptics 350-50, EOM), and a quarter-wave plate (λ/4). The polarization direction was modulated between 0 and π with a period of 0.2 s. The resulting PL intensity (I), then follows the equation:

$$I(t) = \sum_i (\bar{\mu}_i \circ \bar{E}(t))^2 = A \sin^2(\omega t + \phi) + C$$

where $\bar{\mu}_i$ is the dipole moment of the ith absorbing conjugated segment E is the electric field vector of the excitation light, ω is twice the frequency of rotation of the excitation polarization, ϕ is the phase factor, A is the amplitude of modulation of the fluorescence and C is the minimum emission intensity. The parameters A, ϕ, and C are then obtained by least squares fitting of the time trace. The modulation depth (M),[13] defined as M = A/(A + C), allows the alignment of absorbing chromophores to be quantified. For example, M = 0 implies that there is no preferential direction for the absorbing chromophores while M = 1 implies that all the absorbing segments (dipoles) are aligned, i.e., the polymer is rod-like. (Note that by replacing SBS with a polarizing beam splitter, the change in orientation of the emitted light can also be observed.)

The PL lifetime was measured by replacing the cw laser source with a frequency doubled mode-locked tunable Ti:sapphire laser (Coherent, Mira 900 operating at λ = 900 nm, 76 MHz pulse rate, Fig. 2-d). A Soleil-Babinet compensator (New Focus, 5540) operating as a quarter-wave plate (λ/4) was used to transform the linear-polarized (λ = 450 nm) light into circular-polarized light to allow chromophores in polymers with different orientations can be excited equally. Part of the laser pulse was directed to a Silicon photo-diode which acted as a reference signal while the remainder excited the sample. The SBS reflected 100% of the emitted light to a photon counting GaAsP PMT (Hamamatsu, H7422P-40) allowing a time resolution of ~ 300 ps for the system. The DAQ card used for previous experiments was replaced with a time-correlated single-photon counting (TCSPC) card (Becker & Hickl GmbH, SPC-600) to measure the time between excitation and emitted photons. The time intervals between the arrival of emitted photons and the reference signal were used to construct fluorescence decay curves as a function of time. By binning the arrival times of the photons, the fluorescence time trace was also reconstructed.

Finally, to measure the correlation of photons emitted from a single polymer, the temporal separation between consecutive photons was measured by the Hanbury-Brown and Twiss photon correlation experimental scheme[14] using the pulsed laser source.[15] The SBS was used to equally split the PL photons between the two APD detectors, the signal of which was sent to the TCSPC time-correlated single-photon counting (TCSPC) module (Becker & Hickl GmbH, SPC-600) was used to measures the time intervals between adjacent photons. The time intervals were ordered in a histogram to get the interphoton time distribution from which the number of emitters can be obtained.[15,16] Under the condition of short pulse excitation (pulse width << fluorescence lifetime), interphoton times distribute around the multiples of the reciprocal of the repetition rate of the excitation laser. The peak at zero interphoton time represents the number of photon pairs that excited by the same laser pulse and the other peaks being the photon pairs excited by different laser pulses. For a single emitter, the probability of emitting two consecutive photons drops to zero for time intervals shorter than the excited-state lifetime as a single chromophore cannot emit two photons simultaneously (photon anti-bunching). Thus at zero interphoton time there is no peak. For two, three, and four independent emitters, the probabilities are 0.5, 0.67, and 0.75, respectively.

3. HISTORICAL NOTE: THE INITIAL EXPERIMENTS (1999)

The initial single molecule experiments of Prof Fann's group were conducted in 1999 for two months starting from April.[7,17] The first job was to build a confocal microscope in which we could scan the sample. A Nikon (Ellipse 660) optical microscope was used as the base and an old open-loop tube piezoelectric based AFM head with the Z-axis movement disabled (Park Scientific) was attached to the microscope stage. Signal detection was made using a single photon counting module (EG&G SPCM). Short-

chain DOO-PPV was chosen for the experiments.

Raster scanning of the sample was accomplished by using the AFM head's controller. As the peizo-tube was open-loop, there was considerable drift in position over time due to hysteresis. Thus focusing on a molecule and keeping it in focus is not trivial. In order to place a molecule in the laser focus, the laser was first blocked and the voltage manually adjusted to be where we thought we would find the molecule based on the raster scan. After waiting a few minutes for the peizo-tube to move to equilibrium (during this waiting time, the time constant used for data acquisition increased to 300 ms and laser intensity decreased by inserting an neutral density filter), the laser was unblocked and voltage adjusted so as to bring the nearby molecule into the focal point. Once the molecule was found, the laser was again blocked, the intensity increased and time constant decreased. Finally the decay with fluorescence for the molecule was observed for a few minutes at 10 ms resolution. For a many experiments this procedure involved 2 people, one blocking and unblocking the laser beam (Prof. Fann) and the other (JDW) manually increasing and decreasing the voltage.

Published data on MEH-PPV showed that single quench in long chain polymers of 1000's of conjugated segments resulted in a sizable decrease in emission intensity,[4] suggesting efficient exciton migration which was generally assumed to be along the polymer backbone. Our initial results showed that for relatively short polymers, a single quench event had much less effect suggesting inefficient exciton migration along the polymer backbone.

4. RESULTS

The PL spectrum for all the polymers discussed in this paper and the absorption spectra for MEH-PPV in chloroform solution are presented in Fig. 3-a. The PL and absorption spectra of the short chain polymers are clearly blue shifted relative to their long chain polymer analogs. The difference in absorption spectra indicates some bias in the short-chain polymer to shorter segments relative to the long chain polymer. The increased width of the PL spectra of the short relative to long chain polymers is a result of the limited number of conjugated segments in a short chain polymer, e.g., while long chain polymers will have the completed distribution of conjugation lengths, some short chain polymers may lack long conjugated segments thus broadening the distribution. While for long chain polymers, the PL spectrum on individual polymers closely resembles the ensemble average, for short chain polymers, the PL spectrum of individual polymers is considerably narrower than the ensemble average, with the peak position varying from individual as seen in Fig. 3-b. In the following sections, we will summarize the experimental results of 10 years of experiments, considering first short chains containing one to three conjugated segments, moderate length rod-like polymers containing four to six conjugated segments and then finally long chain coiled polymers.

4.1. Short Polymers (one to three conjugated segments)

Fig. 4 displays typical experimental data for a short chain MEH-PPV polymer containing only a few absorbing segments.[6] The PL time trace shown in Fig. 4-a, recorded using 2 APDs, is typical of those seen in our experiment. Changes between intensity levels are abrupt with a drop to zero between intensity changes. For this polymer, two discrete intensity levels can be recognized in its time trace indicating the presence of two active absorbing chromo-

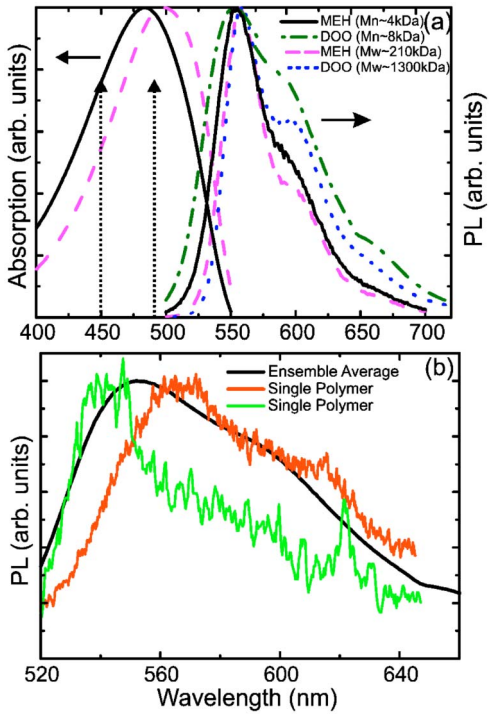

Fig. 3. (a) Absorption and PL spectrum of the polymers in chloroform solution. Dotted vertical lines indicate the wavelengths of laser excitation used. (b) Ensemble average and individual spectra of single rod-like DOO-PPV polymers embedded in the polystyrene matrix (Based on Refs. [6][8][10]).

phores at early times and one active absorbing chromophore at later times. Of the 163 single polymers studied, 40%, 42%, and 18% of the time traces of the single polymers were found to exhibit three, two and one discrete levels, respectively. The drop to zero between changes in intensity is a significant feature of these time traces. Such "on-off" is considered a mark of a single emitter system. This was confirmed by checking the interphoton time statistics of the emission from the polymers. As seen in Fig. 4-a-insert, the height of the zero-interphoton-time peak is very small compared to those of other peaks indicating that there is only a single emitter in this system. The coherent sum of the interphoton time statistics of 69 molecules confirmed that in the majority of polymers there was only one emitting site at a given time.[6] In summary, since the multiple-level behavior seen in the time trace infers that there are about 2-3 absorbing chromophores or conjugated segments, the one emitter feature implies excitons migrate to a single, presumably the lowest energy, emission site before recombining to allow a photon to be emitted.

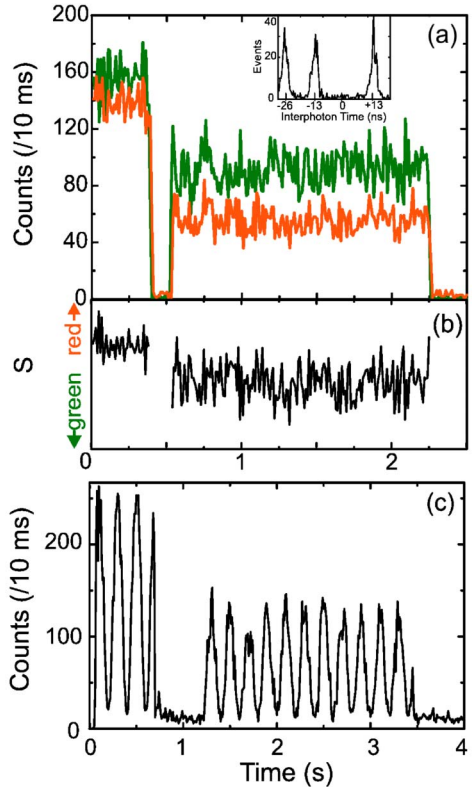

Fig. 4. Typical data for a short chain MEH-PPV polymer containing 2 conjugated segments (a) PL time trace where the PL was split at $\lambda = 550$ nm and directed onto two APDs. Count rates recorded by the APD monitoring the red (green) portions of the spectrum are indicated by red (green) lines. (b) Spectral shift coefficient (S) calculated from the data in (a). (c) PL time trace when the polarization of the excitation light is rotated at 5 Hz. (a-inset) Interphoton time histogram indicating the existence of only one emitting site at a given time. (based on Ref. [6])

This raises the question of whether the excitons are migrating along the backbone or jumping between adjacent conjugated segments (perhaps due to defect induced folding). Fig. 4-c shows a typical polarization spectroscopy result. The fully modulated (M = 1) nature of the time trace indicates that these polymer are indeed have a rod-like conformation and that the excitons are migrating along the polymer backbone.

A final question that needs to be addressed is whether the emitting chromophore changes during the polymers survival time or whether it remains the same before and after a blinking event. This question was addressed by monitoring changes in the spectral composition of the PL and the fluorescence lifetime. Fig. 4-a shows the raw data for a single polymer and Fig. 4-b presents the calculated spectral shift (S) during the polymer's survival time. While S is approximately constant while the emission level is constant, its value is clearly different before and after the blinking event indicating a change in emission site. For this polymer the emitting chromophore at the second step has a higher energy than the one emitting at the beginning of the time trace. Overall, the PL of over 60% of the excited polymers shifted to the green after a blinking event. For 20%, the spectrum shifted to the red. For the remaining 20% the spectra remained unchanged within experimental error suggesting that either the same chromophore resumed emission after the event or the chromophore emitting before and the chromophore emitting after the blinking event were of equal conjugation length. According to exciton theory the transition dipole moment for a conjugated segment increases with the conjugation length of that segment. This increase in dipole moment is reflected experimentally by a drop in fluorescence lifetime. Thus any change in spectrum should also be accompanied by a change in fluorescence lifetime. The ratio of florescence lifetime after and before a blinking event (R) is thus equivalent to a measurement of spectral shift (S). For the 57 spectral changes occurring in 47 polymers, R was less than one for only 5% of the observed polymers.[6] This supports the conclusion that the conjugation length of the emitter after a blinking event is greater than the emitter before a blinking event in the ma-

jority of cases.

4.2. Rod-Like Polymers (four to six conjugated segments)

The effect of polymer length on the number of emission segments was further investigated using short chain Kuhn length DOO-PPV (~24 monomers). This length of polymer was chosen as it is predominately rod-like thus ensuring that all energy transfer within the system is one-dimensional, i.e., along the chain backbone. Based on the theoretical application of the exciton theory to solution measurements,[1] one would expect that excitons would be delocalized over about ~5 monomers on average in this system suggesting that individual DOO-PPV polymers might contain a total of 4 to 6 independently absorbing segments. Fig. 5-a shows an example of the typical time trace for a single DOO-PPV polymer.[8] Note that the intensity drop at ~ 6 seconds is real and not the result of noise as seen in the inset of Fig. 5-a. There are two key observations from this figure. Firstly, similar to the shortest polymers, the decay is clearly step-like with both temporary, e.g., at ~6s and ~45s, and permanent quench events. Secondly, in contrast to the shortest chains, there is no on-off blinking behavior. While for this particular molecule a total of six steps are observed, the most common number of steps was four. Only 20% of the polymers exhibited the expected single step photobleaching or on-off behavior.[7] The lack of on-off blinking suggests that, unlike in the shorter chain case, there is more than one chromophore emitting at a given time. In other words, the ~1ns lifetime of an exciton does not give it sufficient time to migrate to single emission site.

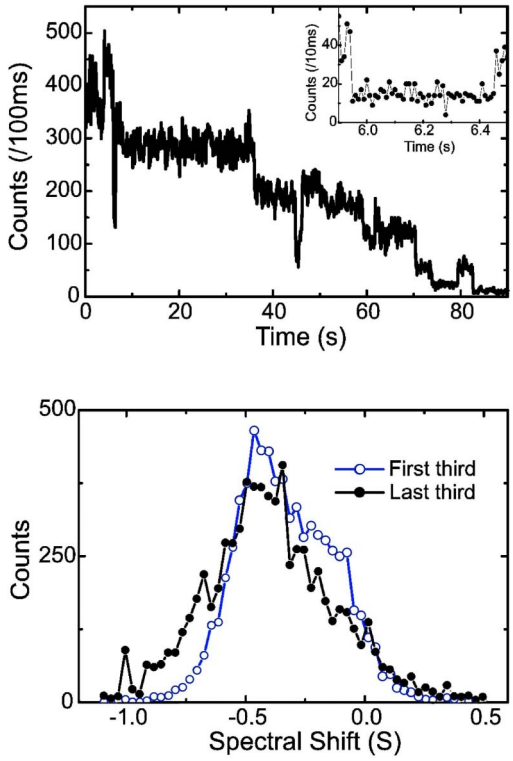

Fig. 5. Typical data for a short DOO-PPV polymer containing ~4-6 conjugated segments. (a) PL time trace (a-inset) Expansion of the scale around 6s to show that the intensity jumps occur abruptly within the 10 ms integration time used in the experiment. (b) Histogram of the spectral shift coefficient (S) for over 30 polymers during the first third and last third of each polymer's survival time. (based on Ref. [8])

The characteristics of the emitting sites on the polymer were further investigated by monitoring changes in the spectral shift coefficient over the survival time for 46 polymers. A feature common to all polymers observed is that, similar to the shortest chains, just as intensity changes are discrete and not gradual, so also is spectral change. However, in contrast to the short chain data, there was little preference for green or red shifts. For 11 polymers, intensity drops were accompanied by a shift to the green. For 15 polymers intensity drops were accompanied by red spectral shift. Six polymers exhibited a combination of green and red-spectral shifts. In 5 polymers, intensity jumps not accompanied by a spectral shift were observed. This lack of spectral shift was confirmed by comparing the spectral shift during the first third of the polymers survival time with that during the last third its survival time. The results are shown in Fig. 5-b. As can be seen in the figure, in contrast to the short chain case, there is no shift towards shorter wavelengths. Combined the above results suggest that absorbing chromophores transfer energy to a few emitters that quench independently.

4.3. Long Chain Polymers (hundreds of conjugated segments)

The PL time traces of two long chain MEH-PPV polymers are shown in Fig. 6-a and c.[9] The time traces of polymers fall into three categories: (1) those that exhibit predominately exponential decay, e.g., Fig. 6-a, (2) those that exhibit predominately abrupt step-like behavior, e.g., Fig. 6-c, similar to that seen for the rod-like polymers (although at a higher intensity) and (3) those whose curves are a combination of the above two behaviors. While for a good solvent such as chloroform, the majority of polymers the time

traces are gradual, for a poorer solvent such as toluene, the majority of time traces are exhibit step like decay.[9] In general, the initial intensity of those time traces that exhibit exponential decay are up to a factor of 10 higher than for those exhibiting step like decay.[18] Typically, exponential decay is what would be expected for a system in which there are many simultaneous emitters while step like decay, as discussed previously, suggests that there are only a few emitters present. The number of emitters in a given system was checked by means of fluorescence correlation spectroscopy. The results for the polymers whose time trace was presented in Fig. 6-a and c are shown in Fig. 6-b and d, respectively. The correlation results confirm that for polymers exhibiting exponential decay, many chromophores emit simultaneously while for those exhibiting step-like behavior there are only a few active emitters at a given time. Taking into account the fact that step like decay is seen most often when MEH-PPV is dissolved in a poor solvent which forces the polymer to tend to fold back tightly on itself, and exponential decay predominates in good solvents where the polymer is expected to extend loosely, the exponential decay is attributed to extended sections of the polymer where one-dimensional exciton migration dominates and the step-like decay attributed to the closely packed sections of the polymer where three-dimensional exciton migration is possible.[5]

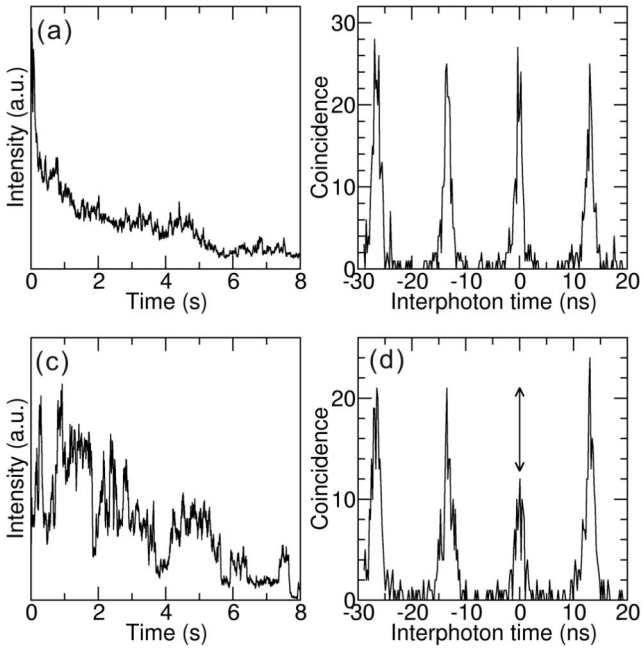

Fig. 6. PL time traces (a and c) and corresponding interphoton arrival time distributions (b and d) for long chain MEH-PPV polymers. (based on Ref. [9])

For comparison with rod-like polymers, the evolution of the spectral shift coefficient over time was also observed for these polymers. In contrast to the rod-like polymers, for the vast majority of polymers observed (269/282), the spectrum clearly shifted towards the green as emission was quenched,[9] regardless of whether the PL time trace was step-like or gradual exponential decay. For polymers whose time trace exhibited exponential-like decay the shift to the green was gradual and continuous. In contrast, in the case of step-like behavior, while over the survival time of the polymer the spectrum shifted to the green, abrupt drops in intensity, did not necessary result in a spectral shift towards the green. Rather individual abrupt drops were accompanied, as in the case of rod-like polymers, by green, red or even no shifts in spectrum.

It is well known that long polymer chains tend to coil back on themselves. While the "tightness" of this structure varies from individual to individual, it has been found to be correlated with solvent choice and the nature of the embedding matrix.[5,19] To obtain insight into the orientation of absorbing chromaphores in the polymer, the polarization of the excitation light was modulated as the PL time trace was recorded. Barbara's group[13] compared the experimentally observed modelation depth (M) for long chain MEH-PPV with that expected from Monte Carlo simulations for six theoretical polymer conformations and showed that the defect cylinder conformation (Fig. 7-e, insert) provided the best fit to the data. Fig. 7-e compares the experimental histogram of the distribution of observed modulation depths for DOO-PPV with the expected histograms for different polymer conformations predicted from the Monte Carlo simulations of Barbara's group.[13] As can be seen from the figure, the conformation of long chain DOO-PPV is also best described by a defect cylinder, similar to MEH-PPV. Further insight into the conformation of individual polymers was obtained by observing changes in M during the survival time of the polymer. Changes in modulation depth for two polymers are shown in Fig. 7.[10] For the polymer lacking abrupt intensity fluctuations, the average modulation depth is ~0.63 and varies only slightly over the life of the polymer. It is uncorrelated with the emission intensity despite intensity changing by an order of magnitude during the section of the time trace shown here. For the polymer whose time trace has abrupt intensity fluctuations, the depth of modulation is less (0.53), and M varies signifi-

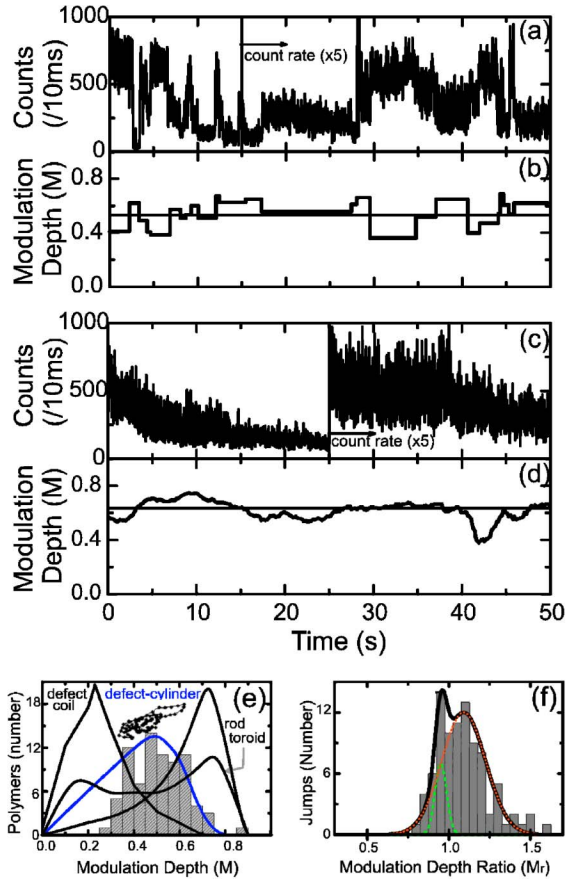

Fig. 7. Results of polarization spectroscopy on single long chains of DOO-PPV polymers.[10] First 50 seconds of the PL time trace (a,c) and variation of modulation depth (M) over time (b,d) for single long chain DOO-PPV polymers when the excitation polarization is slowly rotated. Excitation irradiance is ~1600 W/cm^2. The horizontal line is the root mean square of M (M_{rms}) of the polymer. For the polymer whose time trace is characterized by abrupt steps, M_{rms} = 0.53 and changes drastically during the polymer's survival time. For the polymer characterized by a gradual exponential decay, M_{rms} = 0.633, and is approximately constant as a function of time. (e) Distribution (HM) of the modulation depths (M) from single-molecule polarization spectroscopy for over 79 single DOO-PPV polymers. The value of M plotted is averaged over the lifetime of the each individual polymer. For comparison, the distribution of M values expected for various classes of polymer conformations predicted by simulation are reproduced from Ref. [13] and displayed as solid lines. (f) Histogram of the ratio of depth of modulation ($M_r = M_{low\ intensity} / M_{high\ intensity}$) on either side of abrupt intensity changes for 38 single polymers. Superimposed on the experimental data are the fits to double peaked Gaussian (solid black line). The two dotted lines represent the two sub-species of polymers. (based on Ref. [10])

cantly as a function of time. In addition, M and emission intensity are correlated with shallower modulation at higher intensities. Deeper modulation for the polymer lacking quantized large intensity changes suggests that there is greater anisotropy, i.e., more order, in the orientation of absorption chromophores in the region responsible for gradual changes than for regions responsible for abrupt intensity changes. This point of view was confirmed by monitoring the ratio of depth of modulation ($M_r = M_{low\ intensity} / M_{high\ intensity}$) on either side of the abrupt intensity changes in polymers exhibiting a combination of gradual and abrupt intensity decays. If the alignment of absorption dipoles in the regions of the polymer responsible for abrupt fluctuations in intensity is relatively anisotropic compared to regions responsible for gradual decay, then a sudden drop in intensity should be correlated with an increase in modulation depth. Conversely, a sudden increase in intensity should be accompanied by a corresponding decrease in the modulation depth. As seen in Fig. 7-f the results were bimodel. The best fit suggest that while in 93% of polymers, there is a more isotropic arrangement of absorption dipoles in regions responsible for abrupt intensity fluctuations than in the regions responsible for gradual intensity changes.

5. A PHENOMENOLOGICAL PICTURE OF THE POLYMER

Fig. 8 prevents a schematic picture of the polymer and the changes it experiences that is consistent with the spectral quenching behavior and orientation data presented in the previous sections. Fig. 8-a illustrates the situation of the whole polymer before any quenching event. While the polymers overall shape is defined well by a defect-cylinder, there are both areas of loose packing in which chain segments are well separated and thus exciton migration is predominately one dimensional, as well as sections in which the chains are tightly packed allowing for three dimensional energy transfer. Fig. 8-b presents an expanded view of a part of the chain in an area of loose packing. The emission behavior can be understood by first considering the short chain MEH-PPV system consisting of two to three conjugated segments. (The case of a short polymer with only one conjugated segment is trivially single step on-off blinking with no energy transfer.) The short chain MEH-PPV results suggest that two or three conjugated segments make up a functional unit that is similar to a typical donor-acceptor system. For example, consider the section of the polymer: red (conjugation length 7)-green (conjugation

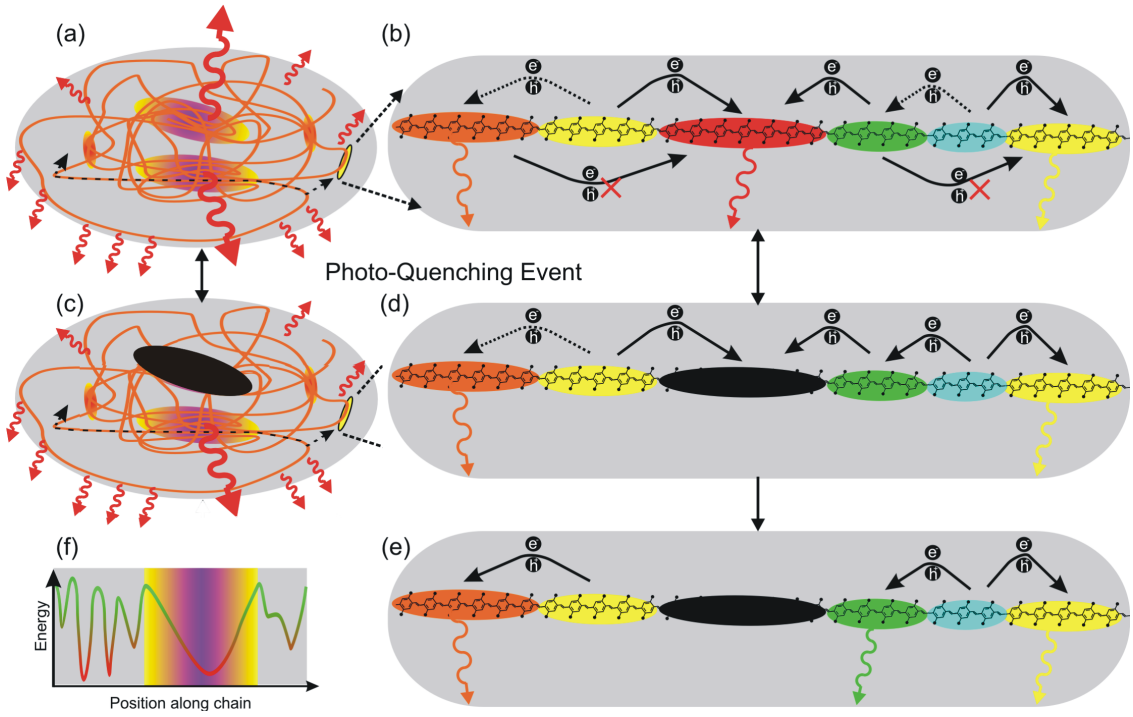

Fig. 8. Schematics illustrating proposed morphology, exciton migration and PL in a long chain PPV derivative polymer under low power continuous illumination. (a & b) Polymer conformation before any photobleaching occurs. (a) The light gray background indicates areas in which exciton migration is one-dimensional, while the colored background indicates areas in which exciton migration is 3 dimensional. The weight of the squiggly lines representing photons reflects the intensity of emission from that section of the polymer. (b) Magnified view of a short section of the extended polymer. (c) Emission of polymer immediately after quench events in the polymer's tightly packed and loosely packed regions. (d) Emission of polymer immediately after a quench event in the extended region. (e) Emission of polymer 100 ms after a quench event in the extended region. (f) Energy landscape of the polymer indicating depths of energy funnels.

length = 4) in Fig. 8-b. Initially, before any quenching event, the 2 chromophores, i.e., donor and acceptor, are absorbing light (Fig. 4-a, from 0 to 0.5 s). The resulting excitons then migrate (via Forster energy transfer) to the longest conjugated segment, i.e., acceptor, where they are emitted (Fig. 4-a-inset, from 0 to 0.5 s). As the acceptor has a much higher probability of being found in an excited state than the higher energy donor, it is preferentially photobleached. After a photo-bleaching event, there is a short time in which no emission occurs (Fig. 4-a from 0.5 to 0.6 s). Presumably, this is due to excitons continuing to migrate to bleached segment and undergoing non-radiative decay (Fig. 8-d). After a period of a ~100 ms, emission resumes: generally at a longer wavelength (Fig. 4-b) and lower intensity (Fig. 4-a from 0.6 to 2 s). This suggests a relatively slow conformational or chemical change that inhibits this exciton migration from the donor to the acceptor (Fig. 8-e). Alternatively, for a minority of cases in our sample, the intensity recovers (temporary quench) and the spectral shift returns to its original value suggesting that the polymer has returned to the situation diagrammed in Fig. 8-b. This view is supported by the blue shift seen in the ensemble measurements of short chain MEH-PPV during photo-bleaching. While this accounts for the behavior of the majority of polymers in the sample, in 18% of the polymers studied, the PL time trace was characterized by emission at a single level: suggesting either the existence of only one conjugated segment or the lack of any conformational change following a photo-bleaching event.

While the short chain MEH-PPV experiment showed classical donor-acceptor behavior, the slightly longer DOO-PPV containing 4-6 conjugated segments did not exhibit such behavior. While the polymer exhibited abrupt intensity fluctuations, there was no blinking and little or no

spectral shift during the survival time of the polymer. Considering again Fig. 8-b, on the one hand, good spectral overlap and proximity allows for efficient exciton migration from shorter to longer adjacent conjugated segments via Forster energy transfer mechanism. On the other hand, inefficient spectral overlap inhibits exciton migration from longer to shorter segments and the lack of proximity hinders migration to the global minimum due to the existence of higher energy intermediate sections. For the six conjugated segments in Fig. 8-b, while all six segments absorb light, the resulting excitons migrate to three different segments before emission. Fig. 8-d illustrates the results of a quench event in which the longest conjugated segment is photo-bleached resulting in a sudden drop in PL intensity and an abrupt spectral shift to the blue. From the schematic it can be seen, that for small number of conjugated segments, there is little reason favor the longest of the emitting segments being photobleached. Thus the spectral shift seen for a given intensity drop may thus be red, e.g., yellow chromophore photo-bleaches; blue, e.g., red chromophore photo-bleaches, or nearly absent, e.g., orange chromophore photo-bleaches. Such a photo-bleaching event may be (1) temporary, e.g., Fig. 5-a 75 to 80 s, where the intensity recovers, (2) permanent, e.g., Fig. 5-a 85 s, where there is no recovery or where after a short period of time, typically of the order of a few hundred milliseconds (cf. Fig. 5-a-inset at 6s) there is a partial recovery of the emission intensity. The latter suggests a conformation change that inhibits exciton migration to the segment allowing emission to commence from elsewhere in the polymer (Fig. 8-e).

These short chain results allow us to identify the extended loosely packed sections of the polymer, i.e., areas in which energy transfer is one-dimensional, as being the source of the gradual intensity decay (Fig. 6-a) with numerous simultaneous emitters (Fig. 6-b). Thus, the tightly packed areas of the polymers, i.e., areas in which energy transfer is three-dimensional, are identified as the source of the large abrupt intensity fluctuations (Fig. 6-c) with simultaneous emitters (Fig. 6-d). The whole polymer contains with numerous extended sections and a few tightly packed regions. Throughout the polymer conjugated segments absorb light. In the tightly packed regions, absorption may be less efficient (seen in the weaker PL observed for long polymers whose time traces are dominated by abrupt intensity fluctuations relative to those whose decay is gradual) and excitons migrate efficiently to a single emitting site where they are emitted. A single quench event, e.g. Fig. 6-c at 4s, darkens the whole section (Fig. 8-c). This quench event can be either temporary or permanent. However, there is no partial recovery, i.e., change to a new emission site, as in the short-chain polymers. We believe this is due to the tightly packed nature of the region and the existence of three-dimensional exciton migration which makes conformational change difficult and quite possibly ineffective in presenting exciton migration.

Fig. 8-f is a schematic of the energy landscape of the polymer across the yellow line in Fig. 8-a. The fact that the spectral shift data for long chain MEH-PPV[9] has a similar value for long-chain polymers irrespective of the nature of their PL time traces suggests that the energy level of the emitting segment in the tightly packed region is not significantly below the energy level of the longest chromophores in the extended regions. While in the extended sections there are numerous narrow wells into which an exciton can be localized, in the tightly packed regions, there is only a single broad energy well due to the existence of three-dimensional energy transfer.

Finally the modulation data provides additional information about the orientation of absorbing segments. While the depth of M suggests that the orientation of absorbing segments is anisotropic for all polymers, the fact that the modulation is deeper for extended chains, suggests that in the tightly packed regions the orientation of absorbing dipoles more isotropic than in the extended chains. This may be the result of the spin-coating process in which the centrifugal force may tend to stretch the extended regions of the polymers more easily than the tightly packed cores.

6. CONCLUSIONS AND FUTURE DIRECTIONS

In this paper photo-quenching has been used to investigate the structure and exciton migration in single polymers of the PPV derivative polymers MEH-PPV and DOO-PPV. Based on the data, phenomenological model based on the polymer as a collection of conjugated segments has been developed.

Due to structural differences, different types of conjugated polymers should have different conformations, conjugated lengths, and so on. Our work demonstrated some methods to characterize these important properties of conjugated polymers. This approach is well suited to the study of all luminescent conjugated polymers and could also be employed to provide greater insights into the effects of chain-length and side-groups. We note that single molecule techniques have been applied to investigate poly-

fluorene,[20] ladder type poly(para-phenylene),[21] and polythiophene.[22]

Finally, in the work described here, we have focused the majority of discussion on the dynamics of intrachain excitons. It is, however, also very important to understand the dynamics of interchain excitons as they are inevitable in both PLEDs and solar cells. We believe this is important future work. Before his death, Prof. Fann had started to study them by ensemble experiments[23] and along with some initial single-molecule experiments (unpublished).

Received May 14, 2010.

REFERENCES

1. Chang, R.; Hsu, J. H.; Fann, W. S.; Liang, K. K.; Chang, C. H.; Hayashi, M.; Yu, J.; Lin, S. H. Chang, E. C.; Chuang, K. R.; Chen, S. A. *Chem. Phys. Lett.* **2000**, *317*, 142.
2. Collini, E.; Scholes, G. D. *Science* **2009**, *323*, 369-373.
3. Hsu, J. H.; Mayashi, M.; Fann, W. S.; Rothberg, L. J.; Perng, G. Y.; Chen, S. A. *J. Phys. Chem. B* **2002**, *106*, 8582
4. Yu, J.; Hu, D.; Barbara, P. F. *Science* **2000**, *289*, 1327.
5. Huser, T.; Yan, M.; Rothberg, L. J. *Proc. Natl. Acad. Sci. USA* **2000**, *97*, 11187.
6. Lim, T.-S.; Hsiang, J.-C.; White, J. D.; Hsu, J. H.; Fan, Y. L.; Lin, K. F.; Fann, W. S. *Phys. Rev. B* **2007**, *75*, 165204.
7. White, J. D.; Hsu, J. H.; Yang, S.-C.; Fann, W. S. *J. Chem. Phys.* **2001**, *114*, 3848-3852.
8. Wang, C. F.; White, J. D.; Lim, T. L.; Hsu, J. H.; Yang, S. C.; Fann, W. S.; Peng, K. Y.; Chen, S. A. *Phys. Rev. B* **2003**, *67*, 035202-1 - 035202-8.
9. Liang, J.-J.; White, J. D.; Chen, Y. C.; Wang, C. F.; Sun, W. Y.; Hsu, J. H.; Fann, W. S.; Peng, K. Y.; Chen, S. A. *Phys. Rev. B* **2006**, *74*(8), 085209.
10. Sun, W.-Y.; Yang, S.-C.; White, J. D.; Hsu, J.-H.; Peng, K.-Y.; Chen, S. A.; Fann, W. S. *Macromolecules* **2005**, *38*(7), 2966-2973.
11. White, J. D.; Sun, W. Y.; Su, S. C.; Hsu, J. H.; Lim, T. L.; Fann, W. S. *J. Lumin.* **2002**, *98*, 45-48.
12. White, J. D.; Hsu, J. H.; Wang, C. F.; Chen, Y. C.; Hsiang, J. C.; Su, S. C.; Sun, W. Y.; Fann, W. S. *J. Chin. Chem. Soc.* **2002**, *49*, 669-676.
13. Hu, D.; Yu, J.; Wong, K.; Bagchi, B.; Rossky, P. J.; Barbara, P. F. *Nature* **2000**, *405*, 1030.
14. Brown, R. H.; Twiss, R. Q. *Nature* **1956**, *177*, 27.
15. Weston, K. D.; Dyck, M.; Tinnefeld, P.; Muller, C.; Herten, D. P.; Sauer, M. *Anal. Chem.* **2002**, *74*,5342-5349.
16. Tinnefeld, P.; Weston, K. D.; Vosch, T.; Cotlet, M.; Weil, T.; Hofkens, J.; Mullen, K.; de Schryver, F. C.; Sauer, M. *J. Am. Chem. Soc.* **2002**, *124*,14310-14311.
17. At that time I (JDW) had just arrived from Xian, China as my Taiwanese wife was pregnant and did not want to give birth in China. (She had, a few years previous, been operated on for breast cancer.) Prof. W. S. Fann graciously arranged for funding to allow me to work in his lab for this time interval.
18. Sun, W.-Y.; Hsu, J.-H.; Yang, S.-C.; White, J. D.; Fann, W.-S. *J. Lumin.* **2002**, *98*, 41-44.
19. Sartori, S. S.; de Feyter, S.; Hofkens, J.; van der Auweraer, M.; de Schryver, F.; Brunner, K.; Hofstraat, J. W. *Macromolecules* **2003**, *36*, 500-507
20. Muls, B.; Uji-i, H.; Melnikov, S.; Moussa, A.; Verheijen, W.; Soumilion, J. P.; Josemon, J.; Mullen, K.; Hofkens, J. *Chem. Phys Chem*. **2004**, *6*, 2286.
21. Muller, J. G.; Lemmer, U.; Raschke, G.; Anni, M.; Scherf, U.; Lupton, J. M.; Feldmann, J. *Phys. Rev. Lett.* **2003**, *91*, 267403.
22. Willets, K. A.; Callis, P. R.; Moerner, W. E. *J. Phys. Chem. B* **2004**, *108*, 10465-10473
23. Huang, Y. F.; Shiu, Y. J.; Hsu, J. H.; Lin, S. H. Su, A. C.; Peng, K. Y.; Chen, S. A. Fann, W. S. *J. Phys. Chem. C* **2007**, *111*, 5533.